NEOPLASIA
www.neoplasia.com

Volume 18 Number 6 June 2016 pp. 371–386 371

A Positive TGF-β/c-KIT Feedback Loop Drives Tumor Progression in Advanced Primary Liver Cancer[1,2]

Andres Rojas*,[3], Pingyu Zhang*,[3], Ying Wang†, Wai Chin Foo‡, Nina M. Muñoz§, Lianchun Xiao¶, Jing Wang†, Gregory J. Gores#, Mien-Chie Hung,††,‡‡ and Boris Blechacz***

*Department of Gastroenterology, Hepatology and Nutrition, The University of Texas MD Anderson Cancer Center, Houston, TX; †Department of Bioinformatics and Computational Biology, The University of Texas MD Anderson Cancer Center, Houston, TX; ‡Department of Pathology, The University of Texas MD Anderson Cancer Center, Houston, TX; §Department of Interventional Radiology, The University of Texas MD Anderson Cancer Center, Houston, TX; ¶Department of Biostatistics, The University of Texas MD Anderson Cancer Center, Houston, TX; #Department of Gastroenterology and Hepatology, Mayo Clinic, Rochester, MN; **Department of Molecular Therapeutics, The University of Texas MD Anderson Cancer Center, Houston, TX; ††Department of Molecular and Cellular Oncology, The University of Texas MD Anderson Cancer Center, Houston, TX; ‡‡Graduate Institute of Cancer Biology and Center for Molecular Medicine, China Medical University, Taichung, Taiwan

Abstract

Hepatocellular carcinoma (HCC) is globally the second most common cause of cancer mortality. The majority of HCC patients are diagnosed at advanced stage disease for which no curative treatments exist. TGF-β has been identified as a potential therapeutic target. However, the molecular mechanisms mediating its functional switch from a tumor suppressor to tumor promoter in HCC and its interactions with other signaling pathways are poorly understood. Here, we demonstrate an aberrant molecular network between the TGF-β and c-KIT pathway that mediates the functional switch of TGF-β to a driver of tumor progression in HCC. TGF-β/SMAD2 signaling transcriptionally regulates expression of the c-KIT receptor ligand (stem cell factor [SCF]) with subsequent auto- and paracrine activation of c-KIT/JAK1/STAT3 signaling. SCF induces TGF-β1 ligand expression *via* STAT3, thereby forming a positive feedback loop between TGF-β/SMAD and SCF/c-KIT signaling. This network neutralizes TGF-β–mediated cell cycle inhibition and induces tumor cell proliferation, epithelial-to-mesenchymal-transition, migration, and invasion. Disruption of this feedback loop inhibits TGF-β tumor-promoting effects and restores its antiproliferative functions. Consistent with our *in vitro* data, we demonstrate SCF overexpression and its correlation to SMAD2 and STAT3 activation in human HCC tumors, advanced tumor-node-metastasis stages, and shorter survival. *CONCLUSIONS:* Canonical TGF-β and c-KIT signaling forms a positive, tumor-promoting feedback loop. Disruption of this loop restores TGF-β tumor suppressor function and provides the rationale for targeting the TGF-β/SCF axis as a novel therapeutic strategy for HCC.

Neoplasia (2016) 18, 371–386

Address all correspondence to: Boris Blechacz, MD, PhD, Department of Gastroenterology, Hepatology and Nutrition, The University of Texas MD Anderson Cancer Center, 1515 Holcombe Blvd., Unit 1466, Houston, TX 77030.
E-mail: bblechacz@mdanderson.org

[1]This work was supported by The University of Texas MD Anderson Cancer Center start-up fund 600700 30 109764 15 (B. B.).
[2]Conflict of interest: None of the authors has competing financial interests or other conflicts of interest in relation to the work described in this manuscript.

[3]Both authors contributed equally.

Received 24 March 2016; Accepted 7 April 2016

1476-5586

http://dx.doi.org/10.1016/j.neo.2016.04.002

Introduction

Hepatocellular carcinoma (HCC) is globally the second most common cause of cancer-related mortality [1]. More than 70% of HCCs are diagnosed at advanced stages not amenable to curative treatments. The multikinase inhibitor sorafenib is the only systemic agent that has demonstrated a survival benefit in advanced-stage HCC that is limited to 2 to 3 months [2]. Novel molecular targeted agents failed to improve outcomes [3]. A better understanding of the molecular signaling networks regulating HCC biology is indispensable for the development of novel therapeutic strategies.

TGF-β signaling through SMAD proteins, known as canonical TGF-β signaling, is a potent tumor suppressor pathway. It is activated through binding of the ligand TGF-β to its cognate receptor resulting in serine phosphorylation and nuclear translocation of transcription factors SMAD2/3. Transcriptional responses to TGF-β are cell type and context specific. Inactivation of TGF-β/SMAD signaling promotes hepatocarcinogenesis [4,5]. Paradoxically, TGF-β1 serum concentrations are elevated in HCC patients and correlate with disease extent and shortened survival [6]. The functional switch of TGF-β to a tumor promoter has been observed in other malignancies; the underlying mechanisms are tumor type specific [7]. TGF-β receptor inhibitors for HCC are being explored in clinical trials, but the mechanisms mediating the TGF-β dysregulation in HCC are poorly understood [8].

c-KIT signaling is initiated through binding of the c-KIT ligand stem cell factor (SCF) to the c-KIT receptor resulting in PI3K/AKT, SRC, and JAK/STAT activation [9]. SCF plays a key role in hepatic regeneration after hepatic injury [10,11]. However, SCF expression in HCC and its role in HCC tumor progression are unknown. Moreover, interactions between TGF-β and c-KIT signaling have not been described.

We aimed to determine the HCC-specific molecular mechanisms mediating TGF-β dysregulation to a driver of tumor progression and characterize the molecular network between TGF-β and c-KIT signaling.

Materials and Methods

Cell Lines and Culture

Human liver tumor cell lines HepG2 (ATCC, Cat. #HB-8065), SNU398 (ATCC, Cat. #CRL-2233), and SNU449 (ATCC, Cat. #CRL-2234) were cultured under standard conditions in Dulbecco's modified Eagle's medium, and Hep3B (ATCC, Cat. # HB-8064) in modified Eagle's medium (10% FBS, penicillin G [100 U/ml], streptomycin [100 μg/ml]). Prior to cytokine treatment, cells were serum starved for 12 hours followed by cytokine incubation under serum-free conditions.

Stably Transduced Cell Lines

Fourth-generation lentiviral vector systems were used for stable transduction with shRNA. Cells were selected with puromycin followed by GFP-directed fluorescence-activated cell sorting. Knockdown was confirmed by quantitative reverse transcriptase polymerase chain reaction (qRT-PCR), immunoblot analysis, and/or enzyme-linked immunosorbent assay (ELISA).

Invasion Assay

Invasion assay was performed as previously described [12]. Invasion was assessed after 48 hours using lightmicroscopic (40×) quantification in three high-power fields (invasion [%] = [mean number of cells invading through Matrigel-coated membrane/mean number of cells migrating through uncoated insert membrane] × 100).

Viability Assay

Cell viability was assessed by manual quantification and methyl thiazol phenyl tetrazolium bromide (MTT) assay. Trypan blue–stained cells were quantified using a hemocytometer. For MTT assay, the CellTiter 96 Non-Radioactive Cell Proliferation Assay (Promega, Cat. #G4000) was used following the manufacturer's recommendations.

BrdU Proliferation Assay

The BrdU cell proliferation assay kit (Cell Signaling Technology) was used according to the manufacturer's recommendations. Absorbance was measured at 450 nM using Synergy H4 hybrid reader (BioTek).

Fluorescence-Activated Cell Sorting

PI-based fluorescence-activated cell sorting was performed as previously described [13]. Cell cycle data analysis was performed using FlowJo software.

Immunofluorescence

Following blocking (1% BSA, TBST), methanol-fixed cells were incubated with primary antibodies overnight at 4°C. Subsequently, cells were incubated with Alexa Fluor 488-/594-conjugated secondary antibodies for 1 hour. Nuclei were stained with 4',6-diamidino-2-phenylindole (DAPI) (1 μg/ml) for 20 seconds. Slides were mounted with SlowFade (Cat. #S36939 Invitrogen) and analyzed by fluorescent microscopy.

Immunoblot Analysis

Whole-cell lysates were analyzed by immunoblot analysis as previously described [14].

ELISA

Human SCF Quantikine ELISA kit (R&D Systems, #DCK00) and the Human TGF-β1 Quantikine ELISA kit (R&D Systems, #DB100B) were used for cytokine quantification following the manufacturer's recommendations.

Chromatin Immunoprecipitation (ChIP)

ChIP-IT Express Enzymatic kit (Active Motif, #53008) was used according to the manufacturer's recommendations. Three micrograms of anti-SMAD2/3, anti-STAT3, or IgG antibody was used per immunoprecipitation.

Transfection

Transfection was performed according to the manufacturer's recommendations using Lipofectamine 2000 (Invitrogen, #11668) for Hep3B cells and Lipofectamine 3000 (Invitrogen, #L3000001) for HepG2 cells.

Luciferase Assay

The luciferase expression vector system pRL-TK (Promega, #E2241) was used for promoter analysis. Firefly and *Renilla* luciferase activities were quantitated using the Dual Luciferase Reporter Assay System (Promega, #E1910).

Microarray Analysis

Microarray data (GEO ID: GSE10186) were obtained from the GEO database. Normalized data were used for detection of genes associated with survival. Genes associated with survival were detected through feature-by-feature Cox PH models in which the gene level was analyzed as the independent variable and the survival status as the

outcome. Genes with a *P* value of < .05 (Suppl. Table 1) were selected for subsequent Ingenuity Pathway Analysis to extract genes involved in the TGF-β signaling pathway. Kaplan-Meier plots were generated for identified genes in the TGF-β signaling pathway. In the Kaplan-Meier plot for each specific gene, samples were divided into two (upregulation and downregulation) groups using the median gene level as the cutoff. A log-rank test was performed to compare the survival rates between two groups.

Migration Assay

Cell migration was assessed using the *in vitro* scratch assay as previously described [15]. At 0, 24, and 48 hours after cell layer disruption, wound width was measured using Image J software.

TUNEL Assay

Cell apoptosis was evaluated by DeadEnd Colorimetric TUNEL system (Promega) following the manufacturer's recommendation. Cells were counterstained with hematoxylin.

Immunohistochemistry

Tissue microarrays and the corresponding clinical information were obtained from US Biomax (Cat. #LV8013) and Imgenex (Cat. #IMH-318 and Cat. #IMH-360). Immunohistochemistry was performed as previously described [14]. Immunohistochemical staining was performed using VECTASTAIN Elite ABC Kit Universal (#PK-7200) and DAB (#SK-4100) substrate KIT (Vector Laboratories, Burlingame, CA). Counterstain was performed with hematoxylin (Vector Laboratories, #H-3404). Two methods were used for quantification: 1) positivity defined as >30% of immunohistochemically positive tumor cells and 2) Allred scoring system [16] adapted for intranuclear pTyr^{705}STAT3, pSer$^{465/467}$SMAD2, and cytosolic SCF. Proportion of positive tumor cells (PS): 0%, 0 points; <1%, 1 point; 1% to 10%, 2 points; 11% to 33%, 3 points; 34% to 67%, 4 points; and >67%, 5 points. Intensity score of positive tumor cells (IS): none, 0 points; weak, 1 point; intermediate, 2 points; and strong, 3 points. The total score (TS) = PS + IS. *Positivity* was defined as TS of more than 2.

Quantitative RT-PCR

Total RNA was extracted using RNAeasy kit (Qiagen, Cat. #74124). cDNA was synthesized using the SuperScript II kit (Invitrogen) and 1 μl added to Power SYBR Green PCR MasterMix (BioRad Cat. #172-5260). Primers (Suppl. Table 1) were added to a concentration of 400 nM. qRT-PCR was performed using the C100 Thermal Cycler (BioRad), and data were analyzed using BioRad CFX Manager.

RNA extraction from human tumor tissue

Paraffin-embedded HCC tumor tissue was obtained through the MD Anderson Cancer Center Pathology tissue bank. Studies were approved by the MDACC Institutional Review Board (IRB #PA13-0674). Tissues were reviewed and macrodissected by a hepatobiliary pathologist (W. C. F.). For RNA extraction, the High Pure RNA Paraffin Kit (Roche, #03270289001) was used according to the manufacturer's instructions.

Plasmid constructs

SCF- and *TGFB*-promoter fragments were amplified from genomic DNA by PCR (Suppl. Table 1) and cloned into position of the BglII/NheI-deleted promoter location of the psiCHECK-2 vector (Promega, #C8021). Plasmid DNA was amplified in DH5α competent cells (Invitrogen, #18258-012) and isolated using PureLink HiPure MaxiPrep Kit (Invitrogen, #K2100-07).

Reagents

TGF-β1 (#101-B1) and SCF (#255-SC-010) were from R&D Systems; TGF-β1 was used at a concentration of 10 ng/ml and SCF at 5 ng/ml, unless otherwise specified. JAK inhibitor I (#420099) and c-Kit inhibitor ISCK03 (#569615) were from EMD Millipore (Billerica, MA); STATTIC (#573099) was from Tocris (Minneapolis, MN). Primers and antibodies are summarized in Suppl. Tables 4 and 5.

Statistical Analysis

In vitro data represent at least three independent experiments using cells from a minimum of three separate isolations and are expressed as means ± standard deviations unless otherwise specified. Differences between two groups were compared using 2-tailed Student's *t* tests. For patient data analysis, continuous variables were summarized using descriptive statistics; categorical variables were tabulated with frequency and percentage. Fisher's exact test and Wilcoxon rank sum test were used to compare categorical and continuous patient characteristics between patients.

Results

SMAD2-activation in HCC and Its Correlation to STAT3-activation and Clinical Parameters

The status of TGF-β pathway constituents in HCC was analyzed using transcriptomic data of 80 HCC patients (Oncomine database, GEO: GPL5474). Using Cox regression analysis, we identified 342 genes associated with clinical outcomes (Suppl. Table 1). Ingenuity Pathway Analysis of these genes demonstrated a correlation between SMAD2 upregulation and SKI downregulation with reduced patient survival (Suppl. Figure 1*A*). SKI protein inhibits canonical TGF-β signaling through inhibition of SMAD2 phosphorylation and as a transcriptional repressor [17,18]. Kaplan-Meier survival analysis confirmed significantly decreased survival in patients with SMAD2 upregulation and SKI downregulation (Figure 1*A*). Subsequently, we analyzed an independent set of matched nonmalignant hepatic and tumor tissues of HCC patients (n = 27) for PAI-1, a transcriptional target of TGF-β/SMAD signaling (Suppl. Figure 1*B*). PAI-1 expression was 3.33-fold (SEM ±0.77) higher in tumor versus normal tissue (P < .0001).

To validate the correlation of TGF-β activation with clinical outcomes, we evaluated nuclear p$^{Ser465/467}$SMAD2 as a surrogate marker of canonical TGF-β signaling activation in HCC tumor samples of an independent third set of 116 patients (Figure 1*B*; patient's characteristics summarized in Suppl. Table 2). SMAD2 activation was significantly higher in advanced HCC (stages III/IV) than early-stage HCC (stages I/II) with a mean Allred score of 4.91 (SEM ±0.26) versus 3.53 (SEM ±0.30) (P = .0007) (Figure 1*C*). Survival was significantly shorter in patients with p$^{Ser465/467}$SMAD2-positive tumors (Suppl. Figure 1*C*).

JAK/STAT3 signaling has a key oncogenic role in hepatocarcinogenesis and HCC tumor progression [19]. We evaluated STAT3 activation in the 116 HCC tumors previously evaluated for p$^{Ser465/467}$SMAD2 (Figure 1*B*). Intratumoral p^{Tyr705}STAT3 levels were considerably higher (P = .02) in advanced than in early-stage HCC with a mean Allred score of 4.72 (SEM ±0.27) versus 3.74 (SEM ±

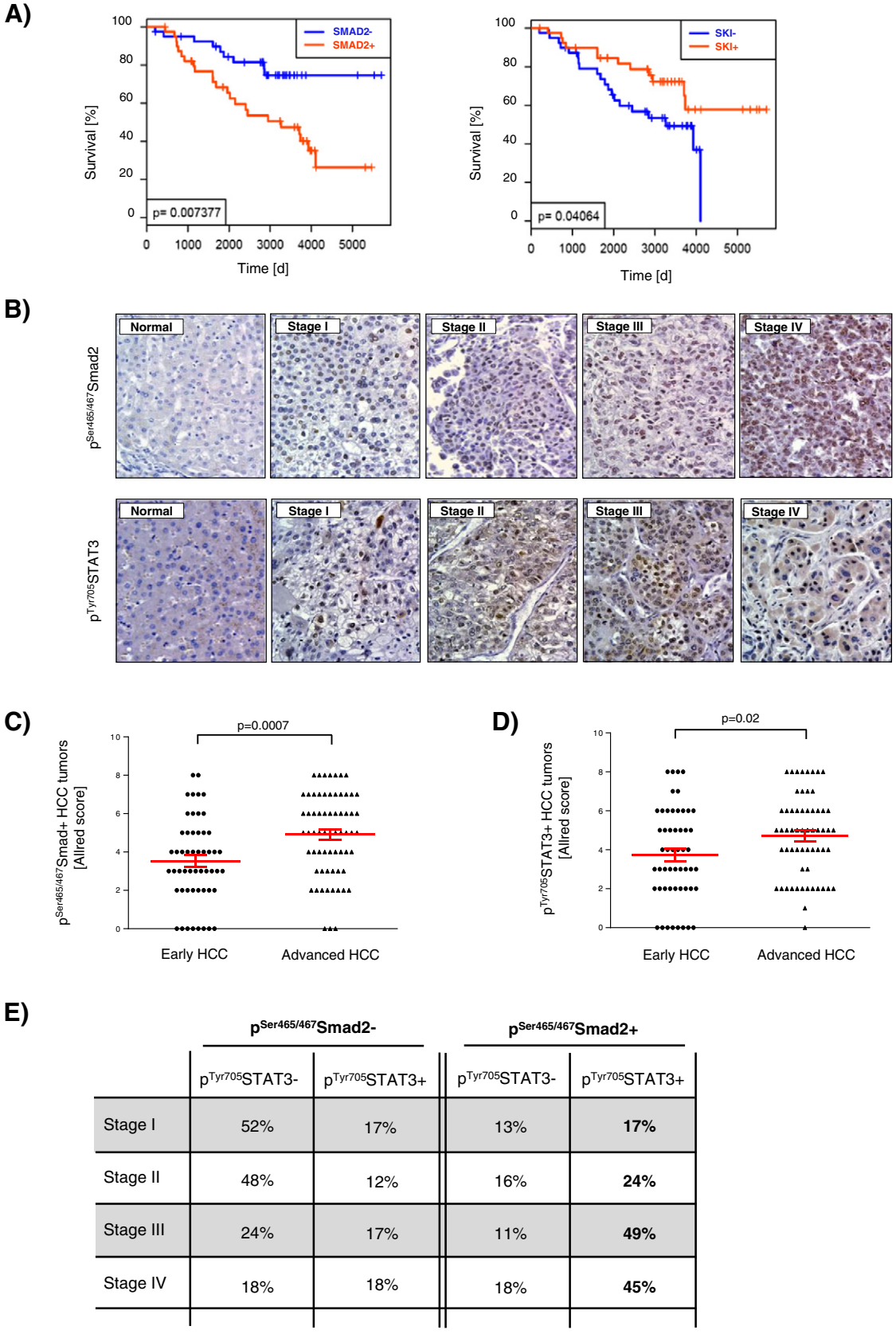

E)

	$p^{Ser465/467}$Smad2-		$p^{Ser465/467}$Smad2+	
	p^{Tyr705}STAT3-	p^{Tyr705}STAT3+	p^{Tyr705}STAT3-	p^{Tyr705}STAT3+
Stage I	52%	17%	13%	**17%**
Stage II	48%	12%	16%	**24%**
Stage III	24%	17%	11%	**49%**
Stage IV	18%	18%	18%	**45%**

0.33) (Figure 1*D*). To determine a potential association between JAK/STAT and TGF-β/SMAD2 signaling, intratumoral $p^{Ser465/467}$SMAD2/p^{Tyr705}STAT3 co-positivity was evaluated (Figure 1*E*). Only 12% to 18% of $p^{Ser465/467}$SMAD2-negative tumors were positive for p^{Tyr705}STAT3. However, 17% to 49% of $p^{Ser465/467}$SMAD2-positive tumors were positive for p^{Tyr705}STAT3. Rates of

$p^{Ser465/467}$SMAD2/p^{Tyr705}STAT3 co-positivity were higher in stages III and IV with 49% and 45% than in stages I and II with 17% and 24%. Correlation analysis for $p^{Ser465/467}$SMAD2 and p^{Tyr705}STAT3 (Suppl. Figure 1*D*) revealed a correlation coefficient $R = 0.51$ (95% confidence interval [CI] 0.28-0.68) in early-stage HCC ($P = .0001$) and $R = 0.72$ (95% CI 0.58-0.82) in advanced-stage HCC ($P < .0001$). Co-immunofluorescence identified intracellular $p^{Ser465/467}$SMAD2/p^{Tyr705}STAT3 co-positivity in HCC tumors (Suppl. Figure 1*E*).

In summary, our results show intratumoral TGF-β/SMAD2 activation in advanced-stage HCC and its correlation with shortened patient survival and STAT3-activation.

Mechanisms of TGF-β1-induced Tumor Progression in Primary Liver Cancer

Physiologically, STAT3 is not a target of TGF-β/SMAD signaling. Based upon the above described correlation between activated STAT3 and SMAD2 in human HCC tumors, we evaluated the association between the two signaling cascades *in vitro*. Importantly, we found that TGF-β1 activated STAT3 only in human liver tumor cells with functional SMAD-mediated TGF-β signaling (Figure 2*A* and Suppl. Figure 2*A*). The TGF-β–mediated activation of STAT3 was predominantly observed in liver tumor cells with sustained SMAD2 phosphorylation in response to TGF-β treatment, whereas no Tyr^{705} phosphorylation of STAT3 was observed in cell lines non- or only transiently responsive to TGF-β treatment in regard to SMAD2 phosphorylation (Suppl. Figure 2*B*). To confirm canonical TGF-β signaling as the STAT3-activating signaling axis, we evaluated the effect of SMAD2 knockdown on TGF-β–induced STAT3 activation. SMAD2 knockdown abrogated TGF-β1–induced Tyr^{705} phosphorylation of STAT3 (Figure 2*B* and Suppl. Figure 2*B*).

To evaluate the functional relevance of TGF-β/STAT3 signaling, we analyzed prooncogenic TGF-β effects [20,21] in parental versus STAT3-knockdown liver tumor cells (Suppl. Figure 2*C*). TGF-β1 induced E-cadherin expression and membranous relocalization in $HepG2^{STAT3\text{-}KD}$ and $Hep3B^{STAT3\text{-}KD}$ cells but not their parental cell lines (Figures 2, *C* and *D*, Suppl. Figure 2*D*). In parental cells, TGF-β1 induced SNAIL1, ZEB1, TWIST, N-cadherin, and vimentin, but STAT3 knockdown abrogated TGF-β1–induced transcription of these epithelial-mesenchymal transition (EMT) markers (Figure 2*C* and Suppl. Figure 2*E*). Unexpectedly, we observed enhanced TGF-β1–induced TWIST transcription in $HepG2^{STAT3\text{-}KD}$ cells, whereas it was abrogated in $Hep3B^{STAT3\text{-}KD}$.

Next, we assessed the effect of TGF-β1–induced STAT3 activation on tumor cell migration and invasion, and the therapeutic efficacy of pharmacologic STAT3 inhibition. Whereas TGF-β potently induced liver tumor cell migration and invasion, this induction was prevented by STAT3 inhibition (Figure 2, *E* and *F*).

Taken together, our results demonstrate that TGF-β activates STAT3 in HCC; this aberrant activation appears to depend on sustained SMAD signaling. The TGF-β/STAT3 signaling network promotes EMT, migration, and invasion of human liver tumor cells.

Antiproliferative Functions of TGF-β/SMAD in Primary Liver Cancer

TGF-β is a known tumor suppressor, but it paradoxically increased cell viability in HepG2 and Hep3B cells. STAT3 inhibition neutralized this paradox TGF-β1 effect (Figure 3*A* and Suppl. Figure 3*A*). TGF-β signaling elicits its tumor-suppressive effects largely by induction of cell cycle arrest and/or apoptosis. However, HCC cells are frequently resistant to TGF-β–induced apoptosis due to overactivation of antiapoptotic signaling pathways [22,23]. Consistent with previous reports [22–24], we did not observe significant TGF-β–induced apoptosis in parental or STAT3-knockdown liver tumor cells (Suppl. Figure 3*B*). However, TGF-β1 inhibited tumor cell proliferation in $HepG2^{STAT3\text{-}KD}$ and $Hep3B^{STAT3\text{-}KD}$, but not in HepG2 or Hep3B cells (Figure 3*B*). Cell cycle analysis revealed that TGF-β–induced G1 cell cycle arrest was restored in $HepG2^{STAT3\text{-}KD}$ in comparison to the parental cell line ($P = .049$) (Table 1). In $Hep3B^{STAT3\text{-}KD}$, TGF-β1 treatment resulted predominantly in G2 cell cycle arrest compared with Hep3B ($P = .006$). Analysis of cell cycle regulatory proteins (Suppl. Figure 3*C*) showed that TGF-β–induced upregulation of $p21^{WAF1/CIP1}$ was maintained in both liver tumor cell lines but considerably enhanced by STAT3 inhibition in Hep3B. Similarly, TGF-β–induced upregulation of $p27^{WAF1/CIP1}$ in HepG2 increased with STAT3 inhibition. Interestingly, TGF-β induced cyclin D1 expression in HepG2, but this induction was inhibited by STAT3 inhibition. TGF-β was recently shown to induce G2/M-phase arrest in Hep3B *via* upregulation of the negative CDK1 inhibitor Wee1 and downregulation of survivin [25,26]. We did not observe an effect of TGF-β on survivin expression in the presence or absence of STAT3 inhibition in Hep3B cells. Whereas we observed TGF-β–induced upregulation of Wee1, this upregulation was inhibited by STAT3 inhibition. However, STAT3 inhibition mediated TGF-β–induced downregulation of cyclin B1 expression.

In summary, TGF-β cell cycle inhibitory and antiproliferative functions are neutralized in human liver tumor cells with aberrant TGF-β–induced STAT3 activation but can be restored by STAT3 inhibition.

Molecular Interactions between TGF-β and c-KIT Signaling in Primary Liver Cancer

To evaluate if TGF-β/SMAD2 induces STAT3 phosphorylation through secondary kinases, we analyzed the effect JAK1 inhibition on TGF-β1–induced STAT3 activation. Complete inhibition of TGF-β–induced Tyr^{705} phosphorylation and nuclear translocation of STAT3, without inhibition of SMAD2 phosphorylation, was achieved by JAK1 blockade (Suppl. Figure 4, *A* and *B*).

In fetal liver cells and human acute megakaryoblastic leukemia cells, the c-KIT ligand SCF activates JAK/STAT3 signaling *via* its cognate receptor c-KIT [27]. Interestingly, we identified TGF-β–induced/SMAD2-dependent SCF expression in human liver tumor cells (Figure 4*A* and Suppl. Figure 4*C*).

To test whether TGF-β activated STAT3 predominantly *via* SCF/c-KIT signaling, TGF-β1–induced STAT3 activation was evaluated

Figure 1. SMAD2 and STAT3 activation in human HCC. (A) Kaplan-Meier plot comparing survival of HCC patients ($n = 80$) based upon SMAD2 and SKI expression. (B) Representative sections of stages I to IV human HCC tissue immunohistochemically stained for $p^{Ser465/467}$SMAD2 (upper panel) and p^{Tyr705}STAT3 (lower panel). (C) Allred scoring system–based quantification of intranuclear $p^{Ser465/467}$SMAD2-positive tumors of HCC patients ($n = 116$); patient's characteristics are summarized in Supplemental Table 2. (D) Allred scoring system–based quantification of intranuclear p^{Tyr705}STAT3-positive tumors of HCC patients ($n = 116$); patient's characteristics are summarized in Suppl. Table 2. (E) Stage-dependent quantification for intratumoral $p^{Ser465/467}$Smad2/p^{Tyr705}STAT3 co-positivity in human HCC tumors ($n = 116$); immunohistochemical positivity defined as >30% of tumor cells per tumor being positive for $p^{Ser465/467}$Smad2 and p^{Tyr705}STAT3.

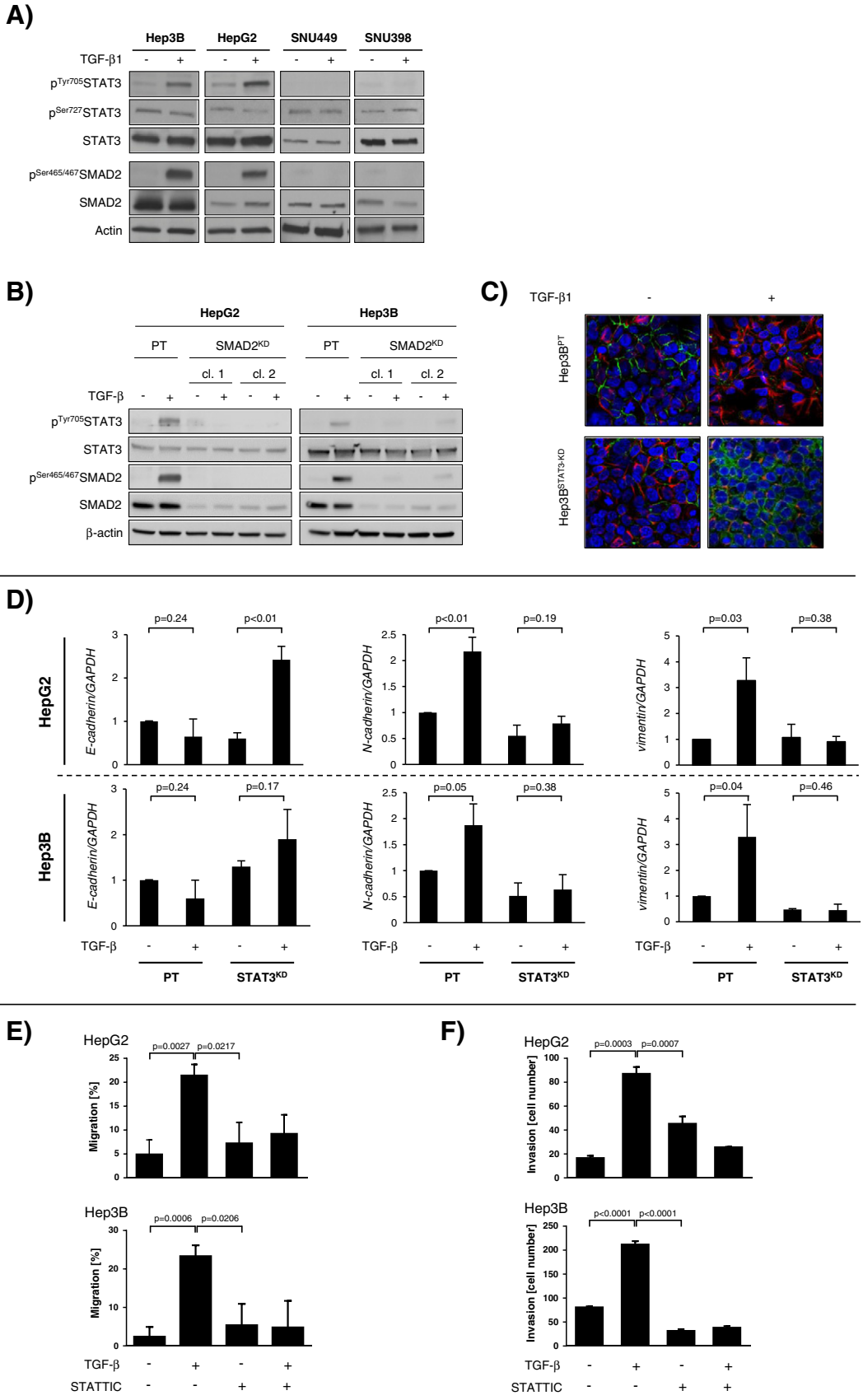

in the presence and absence of the c-KIT inhibitor ISCK03. c-KIT receptor inhibition reduced TGF-β–induced Tyr^{705} phosphorylation of STAT3 (Suppl. Figure 4*D*) and prevented its nuclear translocation (Figure 4*B*). Similarly, SCF knockdown (Suppl. Figure 4*E*) prevented TGF-β1–induced Tyr^{705} phosphorylation of STAT3 in liver tumor cells (Figure 4*C*).

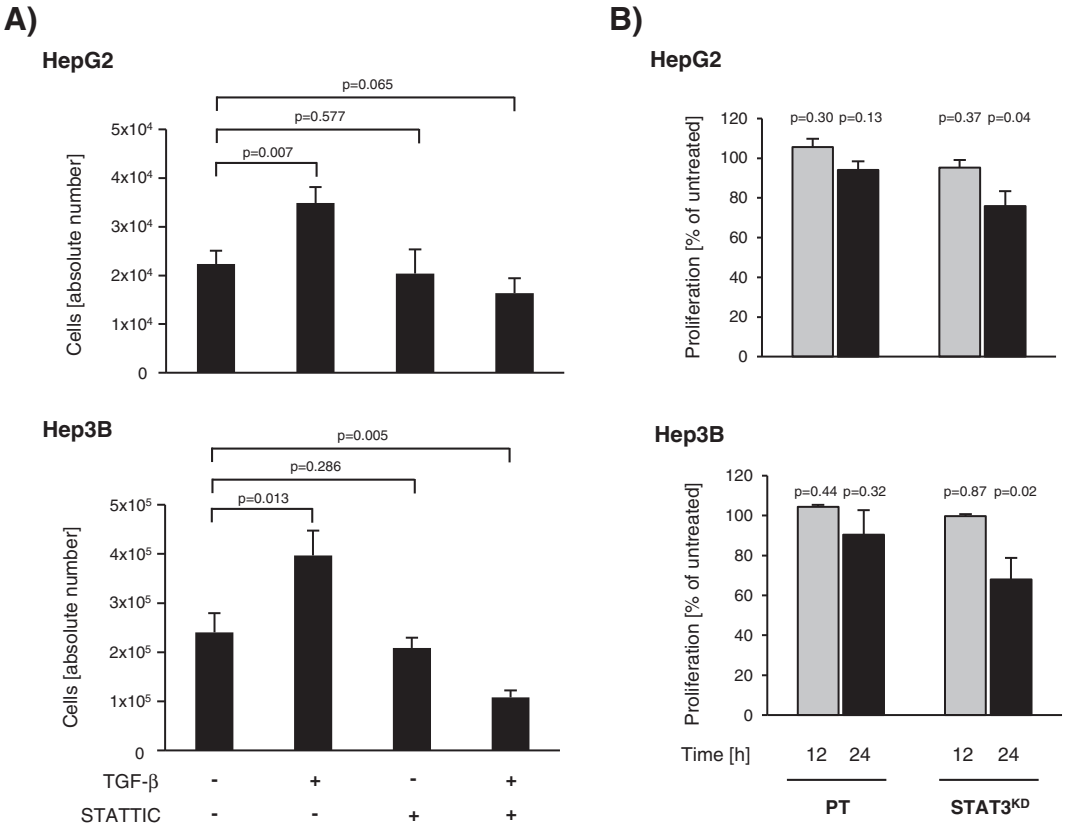

Figure 3. TGF-β antiproliferative functions are neutralized in human liver tumor cells but can be restored by STAT3 inhibition. (A) Liver tumor cell viability analysis after 48 hours of TGF-β1 stimulation (10 ng/ml) ± STAT3 inhibitor STATTIC (5 μM) using trypan blue quantification. (B) BrdU assay of parental and polyclonal STAT3-knockdown liver tumor cells treated with TGF-β1 (10 ng/ml) for 12 and 24 hours. Results are shown as percent of untreated cells (mean ± SEM).

Table 1. Cell Cycle Analysis of TGF-β1–Stimulated Parental and STAT3-Knockdown Liver Tumor Cells.

	PT			$STAT3^{KD}$		
TGF-β	–	+	*P* Value	–	+	*P* Value
HepG2						
Sub G1	1.6 (±2.8)	1.6 (±2.6)	.973	2.0 (±2.1)	1.7 (±1.6)	.839
G0/G1	47.8 (±16.3)	49.4 (±10.4)	.896	45.8 (±14.4)	72.0 (±7.4)	.049
S	20.9 (±14.1)	25.5 (±15.7)	.727	15.9 (±6.3)	10.2 (±9.3)	.435
G2/M	29.6 (±16.8)	23.6 (±3.4)	.578	36.5 (±10.4)	16.2 (±8.1)	.057
Hep3B						
Sub G1	1.5 (±1.7)	2.8 (±3.9)	.628	0.4 (±0.7)	0.7 (±1.1)	.770
G0/G1	51.7 (±6.8)	48.1 (±4.9)	.500	52.7 (±1.7)	27.0 (±2.6)	<.001
S	15.9 (±7.8)	16.3 (±4.5)	.952	20.7 (±4.6)	28.3 (±1.7)	.058
G2/M	30.4 (±5.3)	32.7 (±5.0)	.611	26.0 (±5.4)	44.0 (±1.9)	.006

Cell cycle analysis of TGF-β1–stimulated (12 hours) parental versus polyclonal STAT3-knockdown HCC cell lines using Propidium Iodide (PI)-based fluorescence-activated cell sorting. Results represent the mean ± SD from three independent experiments.

Figure 2. TGF-β1 activates STAT3 and drives tumor progression *via* STAT3. Human liver cancer lines were stimulated for 12 hours with TGF-β1 (10 ng/ml). (A) Immunoblot analysis for TGF-β1 induced activation of SMAD2 and STAT3. (B) Immunoblot analysis for STAT3 activation in parental versus SMAD2-knockdown HepG2 and Hep3B cells. (C) Immunofluorescence analysis for EMT-related proteins vimentin (red) and E-cadherin (green), and nuclear 4',6-diamidino-2-phenylindole (DAPI) stain (blue) in parental versus polyclonal STAT3-knockdown Hep3B cells. (D) qRT-PCR analysis for TGF-β1–induced transcription of EMT markers in parental HepG2 and Hep3B cells, and their polyclonal STAT3-knockdown derivatives. (E) Wound assay for TGF-β1–induced tumor cell migration in the presence or absence of the STAT3 inhibitor STATTIC (5 μM). (F) Invasion assay for TGF-β1–induced tumor cell invasion in the presence or absence of the STAT3 inhibitor STATTIC (5 μM).

In summary, SMAD2-mediated TGF-β signaling transcriptionally regulates c-KIT ligand expression, resulting in STAT3 activation *via* auto- and paracrine stimulation of c-KIT/JAK1.

Molecular Mechanisms of TGF-β-regulated SCF-expression

TGF-β can regulate gene transcription *via* SMAD binding to SMAD binding elements (SBE) within the promoter region of its target genes [28]. We analyzed the SCF promoter-containing 2.4-kb 5′-flanking region of the *SCF* gene for the SBE motif 5′-*AGAC*-3′ [29] and identified seven putative SBE upstream of the *SCF* start codon (Suppl. Figure 4*F*). ChIP assays confirmed TGF-β1–induced SMAD2 binding to the *SCF* promoter in liver tumor cells (Figure 4*D*). For validation, we generated luciferase expression vectors regulated by the full-length *SCF* promoter or *SCF* promoter deletion mutants (Suppl. Figure 4*F*). TGF-β1 stimulation induced luciferase expression in liver tumor cells transfected with the full-length *SCF* promoter; however, sequential deletion of SBE-containing promoter sequences resulted in a gradual decrease in TGF-β–induced luciferase expression (Suppl. Figure 4*G*).

To confirm SMAD2 specificity of *SCF* promoter regulation, parental liver tumor cells and their SMAD2-knockdown derivatives were transfected with the full-length *SCF* promoter luciferase expression vector followed by TGF-β1 stimulation. Whereas TGF-β1 induced luciferase expression in parental liver tumor cells, this induction was abrogated by SMAD2 knockdown (Figure 4*E*).

Our data demonstrate that TGF-β regulates SCF expression through direct transcriptional promoter activation *via* SMAD2 binding to SBE within the *SCF* promoter.

SCF-expression in human HCC and Its Correlation to Clinical Parameters, SMAD2- and STAT3-activation

We analyzed SCF expression in the 116 HCC tumors analyzed before for $p^{Ser465/467}$SMAD2 and p^{Tyr705}STAT3 (Figure 5*A*). SCF was overexpressed at significantly higher rates in advanced versus early-stage HCC with a mean Allred score of 5.38 (SEM ±0.28) versus 3.54 (SEM ±0.40) (P = .0002) (Figure 5*B*). SCF expression was correlated to $p^{Ser465/467}$SMAD2 (P = .007) and p^{Tyr705}STAT3 (P = .06), and clinically to stages T4 (P = .035), N1/Nx (P = .005), and M1 (P = .010) (Suppl. Table 3). Median survival of patients (n = 86) with SCF-positive versus -negative tumors was 29 months versus 79 months (P = .09) (Suppl. Figure 5*A*).

To confirm a potential association between TGF-β/SMAD2 signaling and SCF expression, we evaluated intratumoral $p^{Ser465/467}$SMAD2/SCF co-positivity (Figure 5*C*). Only 7% to 25% of $p^{Ser465/467}$SMAD2-negative tumors were positive for SCF. However, 21% to 50% of $p^{Ser465/467}$SMAD2-positive tumors were co-positive for SCF. Rates of $p^{Ser465/467}$SMAD2/SCF co-positivity were higher in stages III and IV with 42% and 50% than in stages I and II with 21% and 26%. Correlation analysis for $p^{Ser465/467}$SMAD2 and SCF identified a correlation coefficient R = 0.36 (95% CI 0.10-0.57) in early-stage HCC (P = .0081) and R = 0.43 (95% CI 0.21-0.66) in advanced-stage HCC (P = .0003). For validation, we evaluated matching nonmalignant hepatic and tumor tissue of an independent set of HCC patients (n = 36) by qRT-PCR. Consistent with our immunohistochemical analysis, SCF levels were higher in advanced- than early-stage HCC (P = .029) (Figure 5*D*). Correlation analysis for SCF and PAI-1 mRNA (Figure 5*E*) showed a correlation coefficient R = 0.06 (95% CI −0.59 to 0.67) in early-stage HCC (P = .43) versus R = 0.84 (95% CI 0.49-0.96) in advanced-stage HCC (P = .0006). Intracellular SCF/$p^{Ser465/467}$SMAD2 co-positivity was identified in 33% of tumor cells in advanced- versus 19% in early-stage HCC (P = .002) (Figure 5, *F* and *G*).

In summary, SCF is overexpressed in HCC, and its expression correlates with advanced TNM stages and TGF-β/SMAD2 activation. In conjunction with our *in vitro* data, co-positivity for $p^{Ser465/467}$SMAD2 and SCF is intratumoral and intracellular.

Formation of a Positive Feedback Loop between SCF and TGF-β1 in Primary Liver Cancer

Regulation of TGF-β1 expression is cell type specific. TGF-β autoregulation has been described, but its mechanisms are incompletely understood [30]. To test if SCF is a key mediator of TGF-β1 autoregulation, we evaluated TGF-β1 autoregulation in HepG2, Hep3B, $HepG2^{SCF\text{-}KD}$, and $Hep3B^{SCF\text{-}KD}$ cells. Whereas TGF-β1 treatment induced TGF-β1 transcription in parental liver tumor cells, SCF knockdown prevented TGF-β1–induced TGF-β1 transcription (Figure 6*A*). Based upon our data on TGF-β1/SCF-induced STAT3 activation and the recently described STAT3 dependence of TGF-β1 expression during hepatic fibrogenesis [31], we evaluated STAT3 as a mediator of SCF-induced TGF-β1 expression. SCF significantly induced TGF-β1 ligand expression in parental liver tumor cells, but this induction was abrogated by STAT3 knockdown (Figure 6*B* and Suppl. Figure 6*A*).

We analyzed the 5′-flanking region of the *TGFB1* gene for the STAT3 consensus binding motifs 5′-*TT(N4)AA*-3′ and 5′-*TT(N5)AA*-3′ [32]. We identified two putative STAT3-binding sites upstream of the *TGFB1* start codon at positions −4384/−4373 (STB-1) and −5365/−5357 (STB-2) (Suppl. Figure 6*B*). ChIP assays demonstrated TGF-β1–induced STAT3 binding to STB-2 but not STB-1 (Figure 6*C*). We cloned the STAT3 binding site–containing genomic DNA fragments of the *TGFB1* gene into the enhancer position of a thymidine kinase promoter–regulated luciferase expression plasmid (Suppl. Figure 6*B*). Following transfection of these constructs in liver tumor cells, TGF-β1 induced luciferase expression only with plasmids containing STB-2, whereas no activity was observed with plasmids containing only STB-1 (Figure 6*D*).

To confirm SCF as a key inducer of STAT3-mediated TGF-β1 autoregulation, we performed ChIP analysis for TGF-β1–induced STAT3 binding in parental and SCF-knockdown liver tumor cells. TGF-β1 induced STAT3 binding to STB-2 in parental HCC cells but not in $HepG2^{SCF\text{-}KD}$ and $Hep3B^{SCF\text{-}KD}$ (Figure 6*E*). For confirmation, STB-2 STAT3 binding site–containing luciferase constructs were transfected into parental and SCF-knockdown liver tumor cells. TGF-β1 treatment resulted in luciferase expression in parental liver tumor cells but not in $HepG2^{SCF\text{-}KD}$ and $Hep3B^{SCF\text{-}KD}$ (Suppl. Figure 6*C*).

In summary, SCF is the key mediator of TGF-β1 autoregulation in liver tumor cells. TGF-β1/SCF-activated STAT3 binds to the STB-2 regulatory element upstream of the *TGFB1* gene resulting in its induction. Thereby, TGF-β1 and SCF form a positive feedback loop in HCC (Figure 7*A*).

Disruption of the TGF-β/SCF Feedback Loop and Its Therapeutic Potential

Based upon our previous results, we hypothesized that disruption of the TGF-β/SCF signaling loop will inhibit TGF-β–driven tumor progression and restore TGF-β antiproliferative functions in the presence of functional SMAD signaling.

Tumor cell migration of SMAD2-, STAT3-, and SCF-knockdown cells in the absence of treatment did not differ significantly compared with the parental cell lines. However, TGF-β1 treatment significantly induced tumor cell migration of parental liver tumor cells, whereas

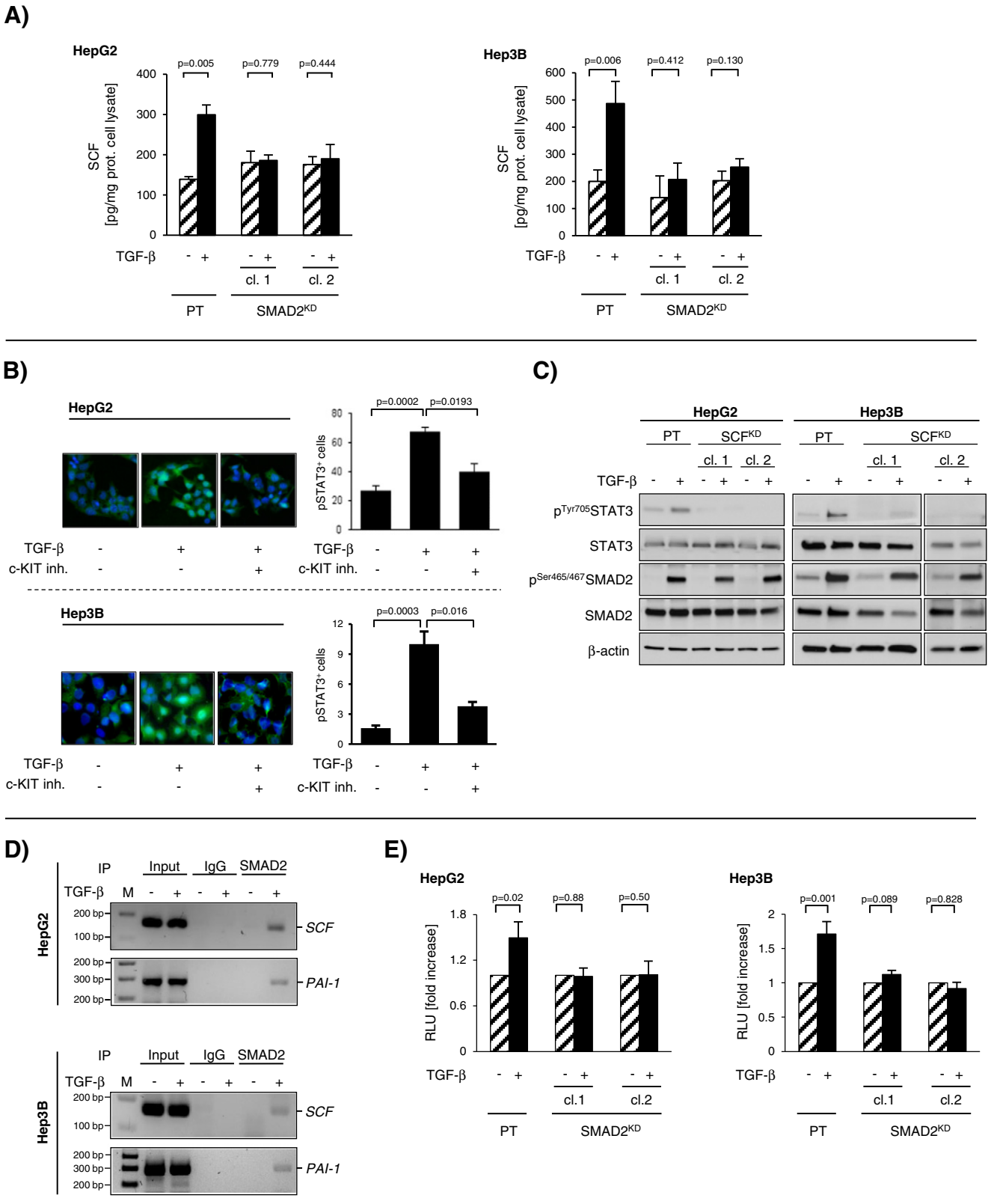

Figure 4. TGF-β transcriptionally regulates SCF expression followed by auto- and paracrine activation of c-KIT/JAK1/STAT3 signaling. HepG2 and Hep3B were stimulated for 12 hours with TGF-β1 (10 ng/ml). (A) ELISA for SCF in the supernatant of TGF-β1–treated parental and SMAD2-knockout liver tumor cells (mean ± SEM). (B) c-KIT dependence of TGF-β–induced STAT3 activation analyzed by immunofluorescence analysis for p^{Tyr705}STAT3 following stimulation with TGF-β1 ± c-KIT inhibitor ISCK03 (5 μM). The bar graphs below show the percent of cells in the immunofluorescence analysis with intranuclear p^{Tyr705}STAT3 accumulation (mean ± SEM of five high-power fields). (C) Immunoblot analysis for TGF-β1–induced STAT3 activation in parental versus polyclonal SCF-knockdown liver tumor cell lines (protein lysates of Hep3B$^{SCF\text{-}KD}$ clone 2 were run on the same gel but noncontiguous). (D) ChIP analysis for SMAD2 binding to the *SCF* promoter following TGF-β1 stimulation; SMAD2 binding to the *PAI-1* gene was used as a positive control. (E) TGF-β1–induced (10 ng/ml, 24-hour stimulation) luciferase activity using *SCF* full-length promoter-regulated luciferase expression plasmids transfected in parental versus SMAD2-knockdown HCC cells.

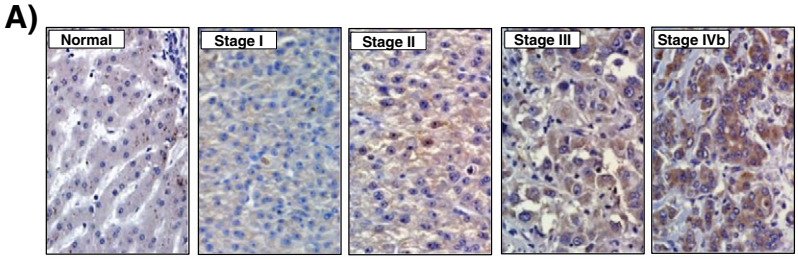

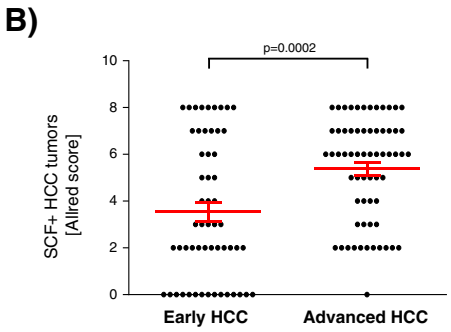

C)

	$p^{Ser465/467}Smad2-$		$p^{Ser465/467}Smad2+$	
	SCF-	SCF+	SCF-	**SCF+**
Stage I	46%	25%	8%	**21%**
Stage II	37%	22%	15%	**26%**
Stage III	30%	7%	21%	**42%**
Stage IV	9%	23%	18%	**50%**

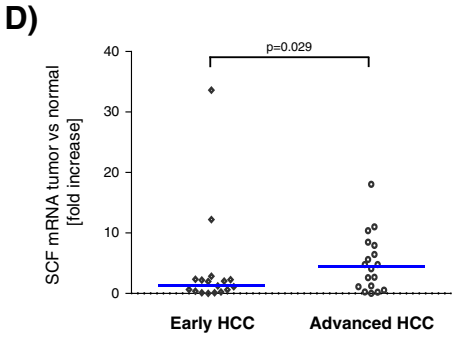

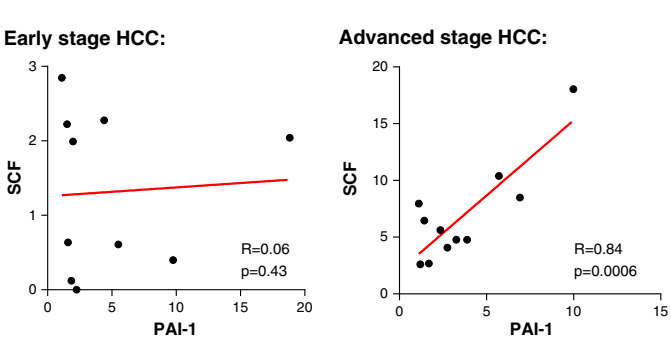

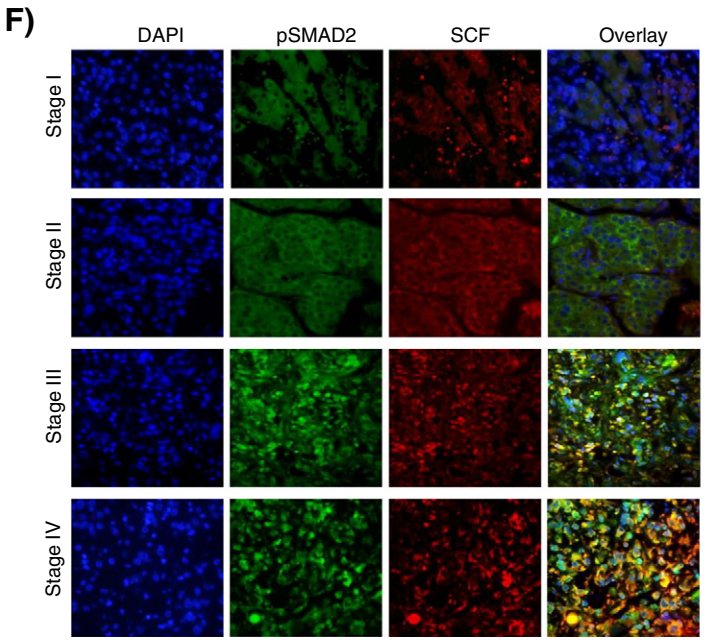

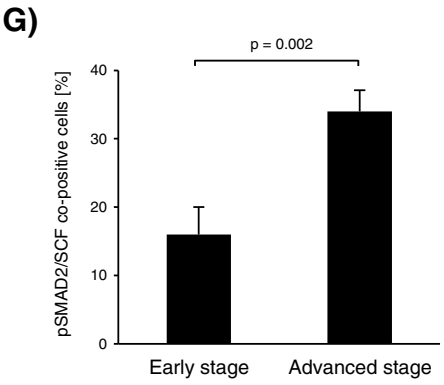

SMAD2, STAT3, and SCF knockdown abrogated TGF-β1–induced migration (Figure 7*B*).

Next, we assessed the effect of SMAD2, SCF, or STAT3 knockdown on TGF-β–induced tumor cell invasion (Figure 7*C*). Interestingly, even though basal levels of tumor cell invasion were higher in $HepG2^{STAT3\text{-}KD}$ and $Hep3B^{SCF\text{-}KD}$ cells, TGF-β1 induced tumor cell invasion only in the parental cell lines. Knockdown of SMAD2, STAT3, or SCF resulted in abrogation or inhibition of TGF-β–induced tumor cell invasion.

Lastly, we assessed restoration of TGF-β antiproliferative functions after disruption of SMAD2, STAT3, or SCF (Figure 7*D*). Consistent with our prior data, no significant antiproliferative effects were observed with TGF-β1 treatment of parental HepG2 and Hep3B cells. As expected, also no significant antiproliferative effects were noted after TGF-β1 treatment of SMAD2-knockdown liver tumor cells. However, TGF-β antiproliferative functions were restored in liver tumor cells after STAT3 and SCF knockdown. Interestingly, TGF-β1 elicited a strong antiproliferative effect even in genetically modified cells with higher basal proliferation rates than their parental cells (HepG2$^{SCF\text{-}KD}$).

Our data show that inhibition of STAT3 and SCF can inhibit the paradoxical tumor-promoting functions of TGF-β and restore its antiproliferative functions. Whereas knockdown of SMAD2 prevents TGF-β–induced tumor cell migration and invasion, it does not restore its antiproliferative effects. This finding is in line with the understanding of canonical TGF-β signaling as the major mediator of TGF-β antiproliferative effects.

Discussion

The multikinase inhibitor sorafenib is the only efficacious systemic therapy, but its survival benefit is limited to 3 months [2]. Novel targeted agents failed to achieve superiority or noninferiority in comparison to sorafenib [33,34]. The TGF-β pathway has been identified as a promising therapeutic target, and TGF-β type I receptor inhibition for HCC is currently being evaluated in clinical trials (NCT01246986, www.clinicaltrials.gov) [8]. However, the molecular mechanisms mediating the functional switch of TGF-β in HCC are poorly understood, and systemic TGF-β inhibition bears risks such as induction of secondary malignancies [35]. TGF-β–induced tumor suppression is mediated by its canonical, SMAD-mediated signaling axis whose inactivation promotes hepatocarcinogenesis [4,5]. Here, we demonstrate TGF-β/SMAD2 activation in advanced HCC and its correlation with shortened patient survival. Our data are supported by recent immunohistochemical and transcriptomic studies demonstrating intratumoral TGF-β/SMAD2 activation in HCC animal models and in human HCC samples, and its correlation with invasive tumor phenotypes [36–40]. Our *in vitro* data confirm the tumor-promoting role of TGF-β in our liver cancer model, and we show that the tumor-promoting role of TGF-β1 is mediated by SMAD2-dependent STAT3 activation. In human tumor samples of patients with advanced-stage HCC, we also find an intratumoral and intracellular positive correlation of SMAD2 and STAT3 activation. STAT3 is a key oncogenic transcription factor in hepatocarcinogenesis and a mediator of metastatic spread and chemotherapy-resistance of HCC cells [19,41]. TGF-β inhibits STAT3 phosphorylation in intestinal epithelial cells, prostate epithelial cells, acute myeloid leukemia blasts, and a murine hepatocarcinogenesis model [42–45], indicating that the here-described TGF-β/STAT3 network is specific for advanced-stage HCC. Interestingly, we observed TGF-β–induced Tyr^{705} phosphorylation of STAT3 only in liver cancer cells with sustained $Ser^{465/467}$ phosphorylation of SMAD2. In several different cancer cell lines, the antiproliferative functions of TGF-β depend on sustained SMAD2 phosphorylation [46–48]. In our liver cancer cell model, though, the antiproliferative functions of TGF-β are neutralized despite sustained SMAD2-phosphorylation. Similar to other groups [48,49], we find induction of cyclin-dependent kinase inhibitors (i.e. $p21^{WAF1/CIP1}$) following prolonged incubation with TGF-β1. However, our data also show upregulation of cyclin B1 in Hep3B cells and TGF-β1–induced upregulation of cyclin D1 in HepG2 cells. STAT3-inhibition downregulates cyclin D1 and cyclin B1, and restores TGF-β–induced cell cycle arrest in our liver cancer model. In human mammary epithelial carcinoma cells and prostate carcinoma cells, it was described that a relative increase of $p21^{WAF1/CIP1}$ to cyclin D1 results in cell cycle arrest [50]. Hence, the paradox of prolonged TGF-β1–induced SMAD2 phosphorylation but neutralized antiproliferative effects in our cell model might be explained by STAT3-induced upregulation of cyclin D1 and cyclin B1—both known transcriptional targets of STAT3 [51].

Several groups reported that malignant hepatocytes that survive TGF-β–mediated cytotoxicity undergo EMT and acquire migratory and invasive properties following the prolonged exposure to TGF-β [8,36,52–55]. In a recent clinical phase 2 trial, it was reported that TGF-β type I receptor inhibition reduces E-cadherin serum concentrations [56]. Consistent with these data, we show that TGF-β induces the transcription of EMT regulators and promotes tumor cell migration and invasion in our liver cancer model. Our *in vitro* data demonstrate that STAT3 inhibition inhibits TGF-β–induced EMT, tumor cell migration, and invasion. Hence, our data suggest that STAT3-targeted therapeutic strategies have the potential to inhibit tumor-promoting effects of TGF-β and restore its tumor suppressor function. STAT3 inhibitors and also agents targeting STAT3-activating kinases (i.e., JAK1/2 and c-KIT) were found to be well tolerated and safe in clinical phase 1 trials [57–59]. This therapeutic approach—curtailing TGF-β's tumor promoter effects and restoring its tumor suppressor function—has several advantages

Figure 5. SCF is overexpressed in advanced HCC and is correlated with pSMAD2 and decreased survival. (A) Representative sections of stage I to IV human HCC tissue immunohistochemically stained for SCF. (B) Allred scoring system–based quantification of SCF-positive tumors of HCC patients (n = 116); patient's characteristics are summarized in Suppl. Table 2. (C) Stage-dependent quantification of intratumoral $p^{Ser465/467}$Smad2/SCF co-positivity in human HCC tumors (n = 116); immunohistochemical positivity defined as >30% of tumor cells per tumor being positive for $p^{Ser465/467}$Smad2 and SCF. (D) *SCF* transcription in tumor versus matching nonmalignant hepatic tissue in an independent set of HCC patients (n = 36). Data were normalized for *GAPDH* and are shown as fold increase in *SCF* mRNA in tumor versus matching nonmalignant hepatic tissue; the blue line represents the median. SCF transcription was significantly higher in advanced- versus early-stage HCC (P = .029). (E) Correlation analysis for intratumoral *PAI-1* and *SCF* mRNA in human HCC tumors. The red line represents the trend line based upon linear regression analysis. Intratumoral *PAI-1* and *SCF* mRNA was significantly (P = .0006) correlated in advanced-stage HCC with a correlation coefficient R = 0.84 (95% CI 0.49-0.96). (F) Representative sections of human stages I to IV HCC tumors evaluated by co-immunofluorescence for SCF and $p^{Ser465/467}$SMAD2 co-localization. (G) Quantification of human HCC tumors (n = 116) analyzed for intracellular SCF/$p^{Ser465/467}$SMAD2 co-positivity. Shown is the percentage of SCF/$p^{Ser465/467}$SMAD2 co-positive tumor cells in $p^{Ser465/467}$SMAD2-positive tumors (median number of cells of five high-power fields per sample).

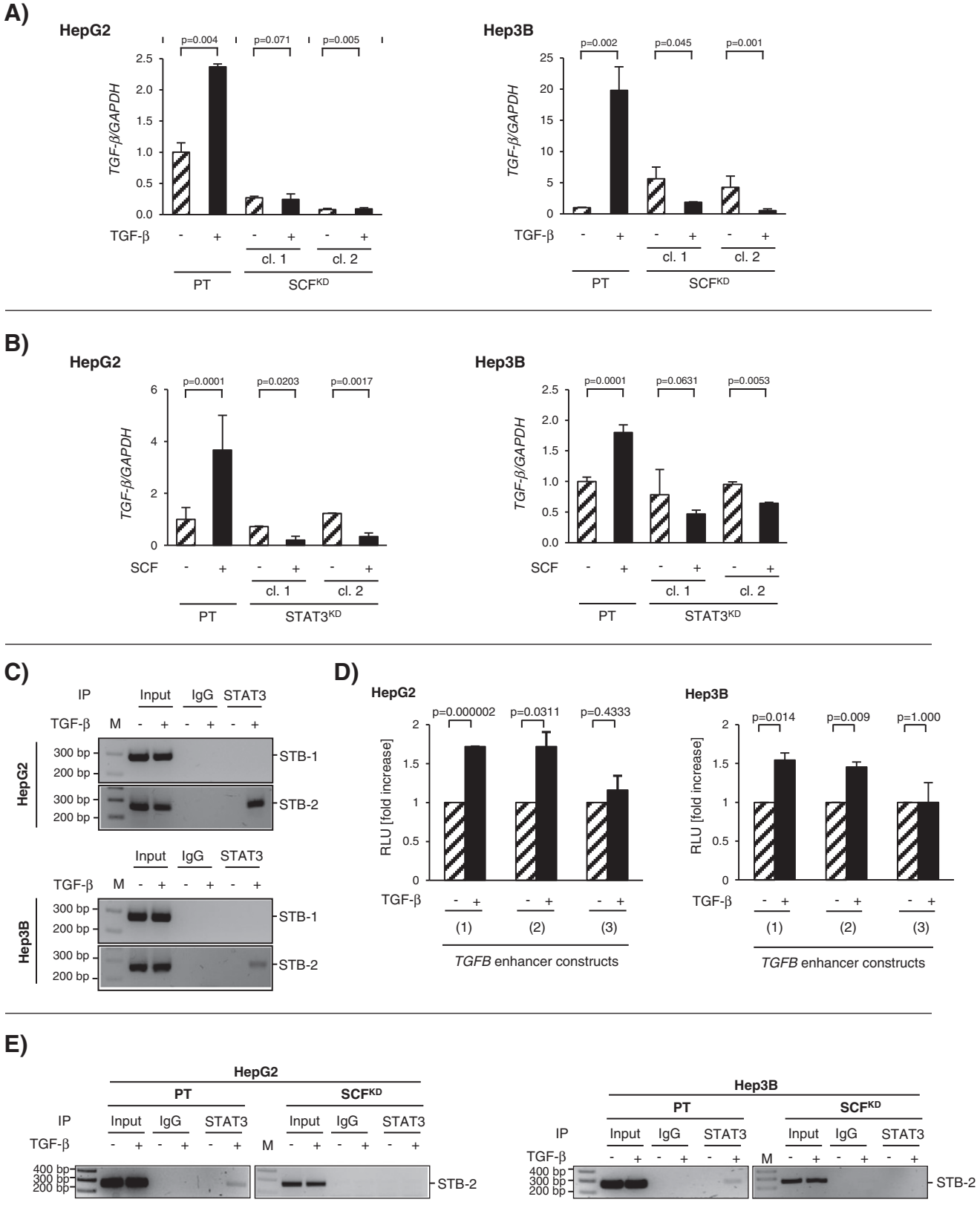

over systemically blocking the TGF-β type I receptor. The potential procarcinogenic effects could be avoided, and elevated TGF-β levels in HCC patients could enhance tumor suppression as an endogenous therapeutic agent. Similarly, Dooley et al. proposed in a recent review article a therapeutic combination strategy aimed at restoration of TGF-β–mediated cytostasis through interference with survival signaling and activation of TGF-β signaling [60].

Mechanisms of STAT3 activation and regulation are cell type and context specific. In preliminary studies using kinase inhibitor approaches, receptor knockdown, and cytokine arrays, we ruled out

other tyrosine kinases (i.e., EGFR, Src, ERK1/2, p38MAPK) and cytokine IL-6 as mediators of TGF-β1–induced Tyr^{705} phosphorylation of STAT3 (Suppl. Figure 7, *A* and *B*) in our liver cancer model. Instead, we identify the c-KIT ligand SCF as the key mediator of TGF-β1–induced STAT3 activation. TGF-β induces SCF expression followed by auto- and paracrine activation of c-KIT/JAK1/STAT3. Interestingly, TGF-β1 is an inhibitor of SCF expression in myelogenous leukemia blasts and hematopoietic progenitor cells [61,62], indicating that TGF-β1–induced SCF expression is specific to liver cancers.

Our data demonstrate that TGF-β regulates SCF expression through direct SMAD2 binding to and subsequent activation of its promoter. Due to the low DNA-binding affinity of SMAD2, SMAD-responsive promoters frequently contain multiple SBE [28,29]. We identified several SBE within the *SCF* promoter and demonstrate SMAD2 binding to the *SCF* promoter. Consistent with observations in the *PAI-1* promoter [63], we find decreasing promoter activity with decreasing numbers of SBE. The SMAD2 specifity of this effect is demonstrated by abrogation of TGF-β–induced *SCF* promoter activation with SMAD2 knockdown. It is likely that additional factors are involved, as SMAD proteins achieve high affinity and selectivity through interaction with other DNA-binding cofactors [28]. Therefore, a SMAD2-knockdown approach was chosen to validate SMAD2 signaling as the mediator of TGF-β–induced SCF expression, as the lack of such cofactors could result in false-negative results even after restoration of SMAD2 activation (i.e., knock-in model with constitutively activated SMAD2). Studies to identify DNA-binding cofactors aberrantly recruiting SMAD2 to the SCF promoter are currently ongoing in our laboratory.

SCF is a critical mitogen for liver regeneration [10,11], but its expression, regulation, and role in HCC are unknown. Our data demonstrate SCF overexpression in HCC and its correlation with advanced TNM stages and shortened patient survival. Consistent with our *in vitro* data, we demonstrate the intracellular correlation between $p^{Ser465/467}$SMAD2 and SCF in human HCC tumors. The correlation of SCF overexpression with the T4, N1, and M1 status of our patient population supports the *in vivo* relevance of our data and the TGF-β/SCF axis as a mediator of TGF-β–mediated tumor progression.

Recently, the need for precision medicine has been recognized to improve outcomes of HCC patients [33,34]. However, the diagnostic benefit of tumor-targeted liver biopsies is limited in HCC by its tumor heterogeneity; noninvasive biomarkers to guide treatment have not been identified [64]. TGF-β1 serum and urine concentrations are elevated in patients with HCC and were found to be predictors of poor outcomes [6,65]. Increased intratumoral SCF expression and SCF serum concentrations were found in patients with ovarian and primary peritoneal carcinoma [66]. Ongoing studies in our laboratory evaluate the diagnostic accuracy of TGF-β/SCF serum analysis to identify subsets of patients whose liver tumors are driven by the TGF-β/SCF/STAT3 axis, thereby providing a noninvasive way to guide targeted therapies.

Recently, it was described that resistance to TGF-β cytotoxicity was mediated by autocrine TGF-β synthesis in fetal rat hepatocytes [67]. Whereas TGF-β autoregulation has been described, its mechanisms are incompletely understood [30]. We characterize the molecular mechanisms of TGF-β1 autoregulation in our liver tumor model and identify SCF/c-KIT as the mediator of its autoregulation. Our data show that TGF-β1/SCF induces STAT3 activation and binding to a regulatory element upstream of the transcription initiation site of *TGFB1* where it acts as a critical regulatory element for TGF-β1 expression. Based upon the location of the STAT3-binding site in relation to the *TGFB1* promoter, and the degree of transcriptional induction following stimulation of the STAT3-binding element, it is likely that STAT3 fulfills an enhancer function in *TGFB1* transcriptional regulation. Our data are supported by recent observations of decreased TGF-β1 expression in IL-$6^{-/-}$ mice and STAT3 dependence of IL-6–induced TGF-β1 expression in hepatocytes [31,68].

In summary, our data show that TGF-β1 and SCF form a positive feedback loop that mediates the functional switch of the TGF-β pathway to a driver of tumor progression in advanced-stage liver cancers. Moreover, we demonstrate that TGF-β–mediated cell cycle inhibition can be restored through disruption of the TGF-β/SCF/STAT3 axis. Interestingly, some of the parental cell lines and their knockdown derivatives displayed differences in their functional behavior under baseline conditions, and the hepatoblastoma and HCC cell lines HepG2 and Hep3B are known to differ in their p53 and Wnt/β-catenin signaling status—two of the most commonly mutated tumor suppressor genes and oncogenic pathways in human HCC [69–71]. However, disruption of the TGF-β/SCF/STAT3 axis resulted in inhibition of tumor-promoting effects of TGF-β1 and restoration of its antiproliferative functions independent of these differences, indicating the therapeutic potential of this strategy. Our current study provides the rationale for targeting the SCF/c-KIT/STAT3-axis, thereby aiding the development of precision medicine for HCC.

Acknowledgements

This work was supported by The University of Texas MD Anderson Cancer Center start-up fund 600700 30 109764 15 (B. B.).

Appendix A. Supplementary data

Supplementary data to this article can be found online at http://dx.doi.org/10.1016/j.neo.2016.04.002.

Figure 6. c-KIT signaling is the mediator of TGF-β autoregulation resulting in a positive feedback loop. (A) qRT-PCR for TGF-β1 ligand transcription in parental and SCF-knockdown liver tumor cells stimulated with TGF-β1; results were normalized for *GAPDH*. (B) qRT-PCR for TGF-β1 ligand transcription in SCF-stimulated parental and STAT3-knockdown HCC cells; results were normalized for *GAPDH*. (C) ChIP analysis of TGF-β1–treated and untreated liver tumor cells immunoprecipitated with an anti-STAT3 antibody followed by PCR using TGF-β specific primers for STB-1 and STB-2; STB-2 also serves as a positive control for STB-1. (D) TGF-β1–induced (10 ng/ml, 24 hours) luciferase activity using luciferase expression plasmids with STAT3 bindings site–containing *TGFB* gene fragments (Suppl. Figure 6*B*) transfected in liver tumor cells. Construct (1) contains STB-1 and STB-2, construct (2) contains STB-2 only, and construct (3) contains STB-1 only. (E) ChIP analysis for TGF-β1–induced STAT3 binding to the STB-2 binding site in parental versus SCF-knockdown liver tumor cells.

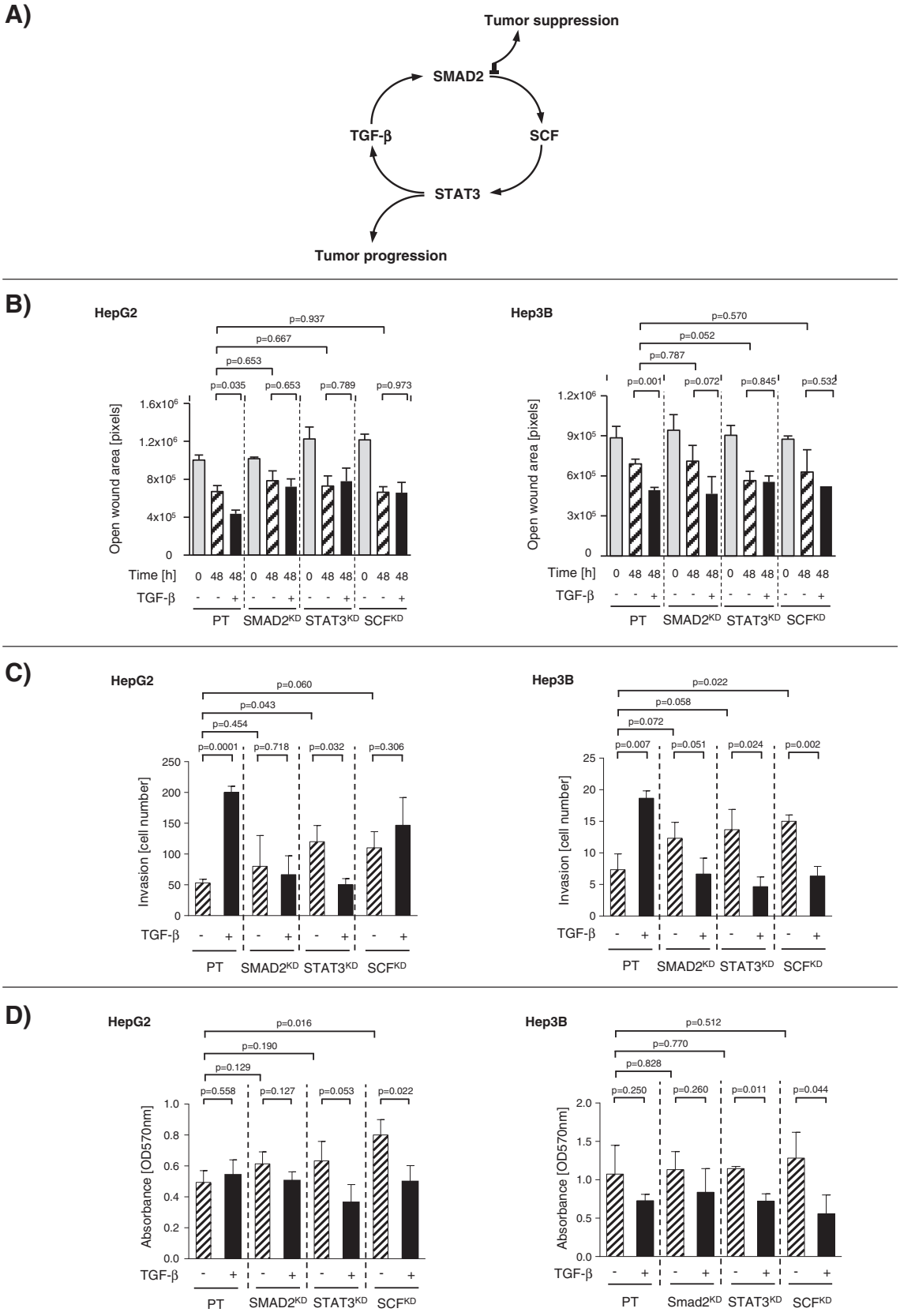

References

[1] WHO (2012). GLOBOCAN 2012: Estimated Cancer Incidence, Mortality and Prevalence Worldwide in 2012. http://globocan.iarc.fr/Pages/fact_sheets_cancer.aspx; 2012.

[2] Llovet JM, Ricci S, Mazzaferro V, Hilgard P, Gane E, Blanc JF, de Oliveira AC, Santoro A, Raoul JL, and Forner A, et al (2008). Sorafenib in advanced hepatocellular carcinoma. *N Engl J Med* **359**, 378–390.

[3] Villanueva A, Hernandez-Gea V, and Llovet JM (2013). Medical therapies for hepatocellular carcinoma: a critical view of the evidence. *Nat Rev Gastroenterol Hepatol* **10**, 34–42.

[4] Kitisin K, Ganesan N, Tang Y, Jogunoori W, Volpe EA, Kim SS, Katuri V, Kallakury B, Pishvaian M, and Albanese C, et al (2007). Disruption of transforming growth factor-beta signaling through beta-spectrin ELF leads to hepatocellular cancer through cyclin D1 activation. *Oncogene* **26**, 7103–7110.
[5] Santoni-Rugiu E, Jensen MR, Factor VM, and Thorgeirsson SS (1999). Acceleration of c-myc-induced hepatocarcinogenesis by Co-expression of transforming growth factor (TGF)-alpha in transgenic mice is associated with TGF-beta1 signaling disruption. *Am J Pathol* **154**, 1693–1700.
[6] Lee D, Chung YH, Kim JA, Lee YS, Lee D, Jang MK, Kim KM, Lim YS, Lee HC, and Lee YS (2012). Transforming growth factor beta 1 overexpression is closely related to invasiveness of hepatocellular carcinoma. *Oncology* **82**, 11–18.
[7] Kang Y, He W, Tulley S, Gupta GP, Serganova I, Chen CR, Manova-Todorova K, Blasberg R, Gerald WL, and Massague J (2005). Breast cancer bone metastasis mediated by the Smad tumor suppressor pathway. *Proc Natl Acad Sci U S A* **102**, 13909–13914.
[8] Giannelli G, Villa E, and Lahn M (2014). Transforming growth factor-beta as a therapeutic target in hepatocellular carcinoma. *Cancer Res* **74**, 1890–1894.
[9] Lennartsson J and Ronnstrand L (2012). Stem cell factor receptor/c-Kit: from basic science to clinical implications. *Physiol Rev* **92**, 1619–1649.
[10] Hu B and Colletti LM (2008). Stem cell factor and c-kit are involved in hepatic recovery after acetaminophen-induced liver injury in mice. *Am J Physiol Gastrointest Liver Physiol* **295**, G45–G53.
[11] Ren X, Hogaboam C, Carpenter A, and Colletti L (2003). Stem cell factor restores hepatocyte proliferation in IL-6 knockout mice following 70% hepatectomy. *J Clin Invest* **112**, 1407–1418.
[12] Shaw LM (2005). Tumor cell invasion assays. *Methods Mol Biol* **294**, 97–105.
[13] Cong R, Das S, Douet J, Wong J, Buschbeck M, Mongelard F, and Bouvet P (2014). macroH2A1 histone variant represses rDNA transcription. *Nucleic Acids Res* **42**, 181–192.
[14] Blechacz BR, Smoot RL, Bronk SF, Werneburg NW, Sirica AE, and Gores GJ (2009). Sorafenib inhibits signal transducer and activator of transcription-3 signaling in cholangiocarcinoma cells by activating the phosphatase shatterproof 2. *Hepatology* **50**, 1861–1870.
[15] Liang CC, Park AY, and Guan JL (2007). In vitro scratch assay: a convenient and inexpensive method for analysis of cell migration in vitro. *Nat Protoc* **2**, 329–333.
[16] Harvey JM, Clark GM, Osborne CK, and Allred DC (1999). Estrogen receptor status by immunohistochemistry is superior to the ligand-binding assay for predicting response to adjuvant endocrine therapy in breast cancer. *J Clin Oncol* **17**, 1474–1481.
[17] Akiyoshi S, Inoue H, Hanai J, Kusanagi K, Nemoto N, Miyazono K, and Kawabata M (1999). c-Ski acts as a transcriptional co-repressor in transforming growth factor-beta signaling through interaction with smads. *J Biol Chem* **274**, 35269–35277.
[18] Prunier C, Pessah M, Ferrand N, Seo SR, Howe P, and Atfi A (2003). The oncoprotein Ski acts as an antagonist of transforming growth factor-beta signaling by suppressing Smad2 phosphorylation. *J Biol Chem* **278**, 26249–26257.
[19] Niwa Y, Kanda H, Shikauchi Y, Saiura A, Matsubara K, Kitagawa T, Yamamoto J, Kubo T, and Yoshikawa H (2005). Methylation silencing of SOCS-3 promotes cell growth and migration by enhancing JAK/STAT and FAK signalings in human hepatocellular carcinoma. *Oncogene* **24**, 6406–6417.
[20] Munoz NM, Upton M, Rojas A, Washington MK, Lin L, Chytil A, Sozmen EG, Madison BB, Pozzi A, and Moon RT, et al (2006). Transforming growth factor beta receptor type II inactivation induces the malignant transformation of intestinal neoplasms initiated by Apc mutation. *Cancer Res* **66**, 9837–9844.
[21] Muraoka RS, Dumont N, Ritter CA, Dugger TC, Brantley DM, Chen J, Easterly E, Roebuck LR, Ryan S, and Gotwals PJ, et al (2002). Blockade of TGF-beta inhibits mammary tumor cell viability, migration, and metastases. *J Clin Invest* **109**, 1551–1559.
[22] Caja L, Sancho P, Bertran E, and Fabregat I (2011). Dissecting the effect of targeting the epidermal growth factor receptor on TGF-beta-induced-apoptosis in human hepatocellular carcinoma cells. *J Hepatol* **55**, 351–358.
[23] Caja L, Sancho P, Bertran E, Iglesias-Serret D, Gil J, and Fabregat I (2009). Overactivation of the MEK/ERK pathway in liver tumor cells confers resistance to TGF-{beta}-induced cell death through impairing up-regulation of the NADPH oxidase NOX4. *Cancer Res* **69**, 7595–7602.
[24] Fernando J, Sancho P, Fernandez-Rodriguez CM, Lledo JL, Caja L, Campbell JS, Fausto N, and Fabregat I (2012). Sorafenib sensitizes hepatocellular carcinoma cells to physiological apoptotic stimuli. *J Cell Physiol* **227**, 1319–1325.
[25] Hashimoto O, Ueno T, Kimura R, Ohtsubo M, Nakamura T, Koga H, Torimura T, Uchida S, Yamashita K, and Sata M (2003). Inhibition of proteasome-dependent degradation of Wee1 in G2-arrested Hep3B cells by TGF beta 1. *Mol Carcinog* **36**, 171–182.
[26] Lee J, Choi JH, and Joo CK (2013). TGF-beta1 regulates cell fate during epithelial-mesenchymal transition by upregulating survivin. *Cell Death Dis* **4**e714.
[27] Weiler SR, Mou S, DeBerry CS, Keller JR, Ruscetti FW, Ferris DK, Longo DL, and Linnekin D (1996). JAK2 is associated with the c-kit proto-oncogene product and is phosphorylated in response to stem cell factor. *Blood* **87**, 3688–3693.
[28] Massague J, Seoane J, and Wotton D (2005). Smad transcription factors. *Genes Dev* **19**, 2783–2810.
[29] Shi Y, Wang YF, Jayaraman L, Yang H, Massague J, and Pavletich NP (1998). Crystal structure of a Smad MH1 domain bound to DNA: insights on DNA binding in TGF-beta signaling. *Cell* **94**, 585–594.
[30] Kim SJ, Angel P, Lafyatis R, Hattori K, Kim KY, Sporn MB, Karin M, and Roberts AB (1990). Autoinduction of transforming growth factor beta 1 is mediated by the AP-1 complex. *Mol Cell Biol* **10**, 1492–1497.
[31] Ogata H, Chinen T, Yoshida T, Kinjyo I, Takaesu G, Shiraishi H, Iida M, Kobayashi T, and Yoshimura A (2006). Loss of SOCS3 in the liver promotes fibrosis by enhancing STAT3-mediated TGF-beta1 production. *Oncogene* **25**, 2520–2530.
[32] Seidel HM, Milocco LH, Lamb P, Darnell Jr JE, Stein RB, and Rosen J (1995). Spacing of palindromic half sites as a determinant of selective STAT (signal transducers and activators of transcription) DNA binding and transcriptional activity. *Proc Natl Acad Sci U S A* **92**, 3041–3045.
[33] Nault JC and Villanueva A (2015). Intratumor molecular and phenotypic diversity in hepatocellular carcinoma. *Clin Cancer Res* **21**, 1786–1788.
[34] Worns MA and Galle PR (2014). HCC therapies–lessons learned. *Nat Rev Gastroenterol Hepatol* **11**, 447–452.
[35] Hawinkels LJ and Ten Dijke P (2011). Exploring anti-TGF-beta therapies in cancer and fibrosis. *Growth Factors* **29**, 140–152.
[36] Bertran E, Crosas-Molist E, Sancho P, Caja L, Lopez-Luque J, Navarro E, Egea G, Lastra R, Serrano T, and Ramos E, et al (2013). Overactivation of the TGF-beta pathway confers a mesenchymal-like phenotype and CXCR4-dependent migratory properties to liver tumor cells. *Hepatology* **58**, 2032–2044.
[37] Mima K, Hayashi H, Kuroki H, Nakagawa S, Okabe H, Chikamoto A, Watanabe M, Beppu T, and Baba H (2013). Epithelial-mesenchymal transition expression profiles as a prognostic factor for disease-free survival in hepatocellular carcinoma: Clinical significance of transforming growth factor-beta signaling. *Oncol Letters* **5**, 149–154.
[38] Yang P, Li QJ, Feng Y, Zhang Y, Markowitz GJ, Ning S, Deng Y, Zhao J, Jiang S, and Yuan Y, et al (2012). TGF-beta-miR-34a-CCL22 signaling-induced Treg cell recruitment promotes venous metastases of HBV-positive hepatocellular carcinoma. *Cancer Cell* **22**, 291–303.
[39] Marquardt JU, Seo D, Andersen JB, Gillen MC, Kim MS, Conner EA, Galle PR, Factor VM, Park YN, and Thorgeirsson SS (2014). Sequential transcriptome

Figure 7. The TGF-β/SCF signaling loop neutralizes TGF-β tumor suppressor function and drives tumor progression *in vitro*. (A) TGF-β/SCF positive feedback loop. TGF-β–activated SMAD2 transcriptionally induces SCF expression *via* direct binding to the *SCF* promoter. SCF expression and secretion result in autocrine and paracrine stimulation of the c-KIT receptor, followed by activation of JAK1/STAT3 signaling. p^{Tyr705}STAT3 translocates to the nucleus where it binds directly to the TGF-β ligand gene, positively regulating its expression. Following activation of secreted TGF-β precursor, it can activate the TGF-β receptor. In addition, TGF-β/c-KIT drive tumor progression *via* STAT3 through neutralization of TGF-β antiproliferative functions and induction of EMT, tumor cell migration, and invasion. Disruption of the TGF-β/c-KIT signaling loop on the level of the SCF/STAT3 axis restores TGF-β tumor suppressor function by inhibition of EMT, tumor cell migration, and invasion, and restoration of its cell cycle inhibitory functions. (B) Migration assay for TGF-β1–induced tumor cell migration in parental liver tumor cells in comparison to their SMAD2-, SCF-, and STAT3-knockdown clones. (C) Invasion assay for TGF-β1–induced tumor cell invasion in parental liver tumor cells, and their SMAD2-, SCF-, and STAT3-knockdown clones. (D) MTT cell viability assay of parental HCC cells versus their SMAD2-, SCF- and STAT3-knockdown clones.

analysis of human liver cancer indicates late stage acquisition of malignant traits. *J Hepatol* **60**, 346–353.

[40] Coulouarn C, Factor VM, and Thorgeirsson SS (2008). Transforming growth factor-beta gene expression signature in mouse hepatocytes predicts clinical outcome in human cancer. *Hepatology* **47**, 2059–2067.

[41] Lee TK, Castilho A, Cheung VC, Tang KH, Ma S, and Ng IO (2011). CD24(+) liver tumor-initiating cells drive self-renewal and tumor initiation through STAT3-mediated NANOG regulation. *Cell Stem Cell* **9**, 50–63.

[42] Wierenga AT, Schuringa JJ, Eggen BJ, Kruijer W, and Vellenga E (2002). Downregulation of IL-6-induced STAT3 tyrosine phosphorylation by TGF-beta1 is mediated by caspase-dependent and -independent processes. *Leukemia* **16**, 675–682.

[43] Walia B, Wang L, Merlin D, and Sitaraman SV (2003). TGF-beta down-regulates IL-6 signaling in intestinal epithelial cells: critical role of SMAD-2. *FASEB J* **17**, 2130–2132.

[44] Starsichova A, Lincova E, Pernicova Z, Kozubik A, and Soucek K (2010). TGF-beta1 suppresses IL-6-induced STAT3 activation through regulation of Jak2 expression in prostate epithelial cells. *Cell Signal* **22**, 1734–1744.

[45] Tang Y, Kitisin K, Jogunoori W, Li C, Deng CX, Mueller SC, Ressom HW, Rashid A, He AR, and Mendelson JS, et al (2008). Progenitor/stem cells give rise to liver cancer due to aberrant TGF-beta and IL-6 signaling. *Proc Natl Acad Sci U S A* **105**, 2445–2450.

[46] Dzieran J, Fabian J, Feng T, Coulouarn C, Ilkavets I, Kyselova A, Breuhahn K, Dooley S, and Meindl-Beinker NM (2013). Comparative analysis of TGF-beta/Smad signaling dependent cytostasis in human hepatocellular carcinoma cell lines. *PLoS One* **8**e72252.

[47] Nicolas FJ and Hill CS (2003). Attenuation of the TGF-beta-Smad signaling pathway in pancreatic tumor cells confers resistance to TGF-beta-induced growth arrest. *Oncogene* **22**, 3698–3711.

[48] Zi Z, Feng Z, Chapnick DA, Dahl M, Deng D, Klipp E, Moustakas A, and Liu X (2011). Quantitative analysis of transient and sustained transforming growth factor-beta signaling dynamics. *Mol Syst Biol* **7**, 492.

[49] Datto MB, Li Y, Panus JF, Howe DJ, Xiong Y, and Wang XF (1995). Transforming growth factor beta induces the cyclin-dependent kinase inhibitor p21 through a p53-independent mechanism. *Proc Natl Acad Sci U S A* **92**, 5545–5549.

[50] Choudhuri T, Pal S, Das T, and Sa G (2005). Curcumin selectively induces apoptosis in deregulated cyclin D1-expressed cells at G2 phase of cell cycle in a p53-dependent manner. *J Biol Chem* **280**, 20059–20068.

[51] Yang CL, Liu YY, Ma YG, Xue YX, Liu DG, Ren Y, Liu XB, Li Y, and Li Z (2012). Curcumin blocks small cell lung cancer cells migration, invasion, angiogenesis, cell cycle and neoplasia through Janus kinase-STAT3 signalling pathway. *PLoS One* 7e37960.

[52] Caja L, Ortiz C, Bertran E, Murillo MM, Miro-Obradors MJ, Palacios E, and Fabregat I (2007). Differential intracellular signalling induced by TGF-beta in rat adult hepatocytes and hepatoma cells: implications in liver carcinogenesis. *Cell Signal* **19**, 683–694.

[53] Gotzmann J, Huber H, Thallinger C, Wolschek M, Jansen B, Schulte-Hermann R, Beug H, and Mikulits W (2002). Hepatocytes convert to a fibroblastoid phenotype through the cooperation of TGF-beta1 and Ha-Ras: steps towards invasiveness. *J Cell Sci* **115**, 1189–1202.

[54] Valdes F, Alvarez AM, Locascio A, Vega S, Herrera B, Fernandez M, Benito M, Nieto MA, and Fabregat I (2002). The epithelial mesenchymal transition confers resistance to the apoptotic effects of transforming growth factor Beta in fetal rat hepatocytes. *Mol Cancer Res* **1**, 68–78.

[55] Nejjari M, Hafdi Z, Gouysse G, Fiorentino M, Beatrix O, Dumortier J, Pourreyron C, Barozzi C, D'Errico A, and Grigioni WF, et al (2002). Expression, regulation, and function of alpha V integrins in hepatocellular carcinoma: an in vivo and in vitro study. *Hepatology* **36**, 418–426.

[56] Giannelli G, Santoro A, Kelley RK, Merle P, Gane E, Douillard JY, Waldschmidt D, Mulcahy M, Costentin C, Lorusso G, Gueorguieva I, Cleverly A, Desaiah D, Lahn MM, Murray N, Benhadji KA, Raymond E, and Faivre S (2013). Phase 2 study of the oral transforming growth factor-beta (TGF-beta) receptor I kinase inhibitor LY2157299. 7th Annual ILCA Conference, International Liver Cancer Association Washington, D.C., USA; 2013.

[57] Ogura M, Uchida T, Terui Y, Hayakawa F, Kobayashi Y, Taniwaki M, Takamatsu Y, Naoe T, Tobinai K, and Munakata W, et al (2015). Phase I study of OPB-51602, an oral inhibitor of signal transducer and activator of transcription 3, in patients with relapsed/refractory hematological malignancies. *Cancer Sci* **106**, 896–901.

[58] Oh DY, Lee SH, Han SW, Kim MJ, Kim TM, Kim TY, Heo DS, Yuasa M, Yanagihara Y, and Bang YJ (2015). Phase I Study of OPB-31121, an Oral STAT3 Inhibitor, in Patients with Advanced Solid Tumors. *Cancer Res Treat* **47**, 607–615.

[59] Verstovsek S, Kantarjian H, Mesa RA, Pardanani AD, Cortes-Franco J, Thomas DA, Estrov Z, Fridman JS, Bradley EC, and Erickson-Viitanen S, et al (2010). Safety and efficacy of INCB018424, a JAK1 and JAK2 inhibitor, in myelofibrosis. *N Engl J Med* **363**, 1117–1127.

[60] Meindl-Beinker NM, Matsuzaki K, and Dooley S (2012). TGF-beta signaling in onset and progression of hepatocellular carcinoma. *Dig Dis* **30**, 514–523.

[61] de Vos S, Brach MA, Asano Y, Ludwig WD, Bettelheim P, Gruss HJ, and Herrmann F (1993). Transforming growth factor-beta 1 interferes with the proliferation-inducing activity of stem cell factor in myelogenous leukemia blasts through functional down-regulation of the c-kit proto-oncogene product. *Cancer Res* **53**, 3638–3642.

[62] Heinrich MC, Dooley DC, and Keeble WW (1995). Transforming growth factor beta 1 inhibits expression of the gene products for steel factor and its receptor (c-kit). *Blood* **85**, 1769–1780.

[63] Dennler S, Itoh S, Vivien D, ten Dijke P, Huet S, and Gauthier JM (1998). Direct binding of Smad3 and Smad4 to critical TGF beta-inducible elements in the promoter of human plasminogen activator inhibitor-type 1 gene. *EMBO J* **17**, 3091–3100.

[64] Blechacz B and Mishra L (2015). Biopsy for liver cancer: How to balance research needs with evidence-based clinical practice. *Hepatology* **62**, 1645.

[65] Tsai JF, Jeng JE, Chuang LY, Yang ML, Ho MS, Chang WY, Hsieh MY, Lin ZY, and Tsai JH (1997). Elevated urinary transforming growth factor-beta1 level as a tumour marker and predictor of poor survival in cirrhotic hepatocellular carcinoma. *Br J Cancer* **76**, 244–250.

[66] Schilder RJ, Sill MW, Lee RB, Shaw TJ, Senterman MK, Klein-Szanto AJ, Miner Z, and Vanderhyden BC (2008). Phase II evaluation of imatinib mesylate in the treatment of recurrent or persistent epithelial ovarian or primary peritoneal carcinoma: a Gynecologic Oncology Group Study. *J Clin Oncol* **26**, 3418–3425.

[67] Del Castillo G, Murillo MM, Alvarez-Barrientos A, Bertran E, Fernandez M, Sanchez A, and Fabregat I (2006). Autocrine production of TGF-beta confers resistance to apoptosis after an epithelial-mesenchymal transition process in hepatocytes: Role of EGF receptor ligands. *Exp Cell Res* **312**, 2860–2871.

[68] Natsume M, Tsuji H, Harada A, Akiyama M, Yano T, Ishikura H, Nakanishi I, Matsushima K, Kaneko S, and Mukaida N (1999). Attenuated liver fibrosis and depressed serum albumin levels in carbon tetrachloride-treated IL-6-deficient mice. *J Leukoc Biol* **66**, 601–608.

[69] Muller M, Strand S, Hug H, Heinemann EM, Walczak H, Hofmann WJ, Stremmel W, Krammer PH, and Galle PR (1997). Drug-induced apoptosis in hepatoma cells is mediated by the CD95 (APO-1/Fas) receptor/ligand system and involves activation of wild-type p53. *J Clin Invest* **99**, 403–413.

[70] Puisieux A, Galvin K, Troalen F, Bressac B, Marcais C, Galun E, Ponchel F, Yakicier C, Ji J, and Ozturk M (1993). Retinoblastoma and p53 tumor suppressor genes in human hepatoma cell lines. *FASEB J* **7**, 1407–1413.

[71] Kan Z, Zheng H, Liu X, Li S, Barber TD, Gong Z, Gao H, Hao K, Willard MD, and Xu J, et al (2013). Whole-genome sequencing identifies recurrent mutations in hepatocellular carcinoma. *Genome Res* **23**, 1422–1433.